Study of lateral distribution of impurities on samples exposed in ASDEX Upgrade using microbeam of ^{3}He and ^{1}H

M Kelemen[1,2*], A Založnik[1], P Vavpetič[1], P Pelicon[1], A Hakola[3], G Meisl[4], M Oberkofler[4], K Krieger[4], S Brezinsek[5], S Markelj[1], the ASDEX Upgrade Team[4] and EUROfusion MST1 Team[a]

[1] Jožef Stefan Institute, Jamova 39, SI-1000 Ljubljana, Slovenia

[2]Jožef Stefan International Postgraduate School, Jamova cesta 39, 1000 Ljubljana, Slovenia

[3] VTT Technical Research Centre of Finland Ltd, P O Box 1000, FI-02044, VTT, Finland

[4] Max-Planck-Institut für Plasmaphysik, Boltzmannst. 2, D-85748 Garching, Germany

[5] Forschungszentrum Jülich GmbH, Institut für Energie- und Klimaforschung Plasmaphysik, Partner of the Trilateral Euregio Cluster, 52425 Jülich, Germany

[a] See the author list of **H. Meyer et al., "Overview of progress in European medium sized tokamaks towards an integrated plasma-edge/wall solution", Nuclear Fusion 57 (2017) 102014.**

***Corresponding author: M. Kelemen**

E-mail address: mitja.kelemen@ijs.si

Abstract

In this paper, we present the use of focused MeV ion beams to study the distribution of deuterium (D), boron (B) and nitrogen (N) on tungsten (W) samples exposed in the divertor region of ASDEX Upgrade tokamak during ^{15}N-seeded L-mode discharges in deuterium and during non-seeded H-mode discharges in helium. In both experiments samples of various surface roughness were exposed and analyzed: W coatings on milled or polished graphite substrates and bulk W samples, ranging from the roughest (milled) to the smoothest (bulk W), to study the effects of surface roughness on deposition profiles of D, B and N. In the case of samples from the ^{15}N experiment, we found that D, N and B are distributed quite homogeneously over the sample on the micrometer scale with some small variation inside the analysed area. The surface densities show strong variations in the poloidal direction, with maximum values slightly above the strike point. The amounts of the retained (D, B, N) were strongly correlated with the surface roughness of the samples, being the highest on the rough samples. Samples originating from the He campaign showed inhomogeneous distribution of impurities with a distinct micro-scale structure, which is most pronounced on pre-damaged W samples, where rough fuzz-like surface is created during the exposure in GLADIS machine. We observe distinct difference in behavior of deposited B profiles from both experiments with higher retention of B in He experiment.

Keywords: Focused ion beams, Deuterium, ^{3}He, Nuclear Reaction Analysis, PIXE

PACs: 29.30.Ep, 25.55.-e, 24. , 29.30.Kv

Introduction

One of the key research areas in the field of plasma-surface interactions is erosion and migration of impurity species and fusion fuel inside of fusion devices. Migration of impurities influences erosion and deposition patterns on plasma facing components and can be an important contributor to fusion fuel retention due to the co-deposition. Two of the most important impurities are nitrogen (N), which is used as a seeding gas to promote radiative plasma cooling and, in the ASDEX Upgrade (AUG) tokamak, boron (B) which is used as a getter material to suppress the oxygen content on tungsten (W) plasma facing components in the tokamak vessel.

Ion beam analytical (IBA) methods with a broad (≈1 mm^2) analysing beam are usually used to provide the information on the surface composition and concentration of impurities on samples exposed in tokamaks [1]. By means of a focused MeV ion beam one can obtain additional information on the lateral distribution of retained fuel and impurities on the micro-meter scale. Here, we are mainly interested in the impurity variation in the poloidal direction [2,3,4].

We present the results of microbeam analyses on samples exposed in the divertor region of the AUG in two different experiments: during ^{15}N-seeded L-mode discharges in deuterium and during non-seeded H-mode discharges in helium. In this way, the effect of specific operational conditions (plasma gases and discharges) and surface roughness (different sample compositions) on the deposition and erosion profiles were studied. We determined the distribution of retained plasma fuel (deuterium (D)), applying nuclear reaction analysis (NRA) with ^{3}He ions, and two light impurities, boron (^{11}B) and nitrogen (^{15}N) also by NRA using proton microbeam. Detection of heavier metallic impurities was performed by using particle induced X-ray emission spectroscopy. The surface roughness of the set of studied samples spans from mirror like polished surface (nm range) up to rough ones with μm features on the surface. We aimed to see if there is any correlation between surface features (originating from surface roughness or scratches) and distribution of impurity deposition and fuel. This essentially can determine if local areas in a divertor are swapped from erosion to deposition-dominated regime under combined fuel and impurity bombardment which has implications on the W source strength and retention in the divertor.

2. Experimental set-up

The analysed samples were, during the plasma discharge, mounted on a divertor manipulator arm of AUG machine which enables exposure of several small samples to divertor plasmas in the vicinity of the low-field side (outer) strike point [5]. One set of samples was exposed during ^{15}N-seeded L-mode discharges in D [6]. Altogether 5.3x10^{21} ^{15}N atoms were injected during 5 L-mode D discharges, described in details in Ref. [6]. ^{15}N was used as the tracer since its natural abundance is only 0.4%, and thus for the analyses contamination from the surrounding air is negligible. Overall, 6 samples with three types of microstructure were analysed, originating from below (in the private flux region) and above strike point [5] labelled as position 2 and 3 respectively (Figure 1a). . The first type consists of 100 nm of W deposited on milled (rough) graphite (samples M2, M3). The second type

consists of 100 nm of W deposited on polished fine grained graphite (samples P2, P3). The third type consists of mirror polished bulk W (samples W2, W3). With such a selection of the samples we covered a large range of surface roughness where milled being the roughest (R_a> 1 μm) and bulk W being the smoothest (R_a< 1 μm). Details of the composition and microstructure are given in Table 1.

The second set of samples was exposed during H-mode discharges in He, more details of the experiment can be found in [7,8]. Now, 3 samples from around the strike point of the experiment were selected for analyses, one of them being bulk W sample (labelled as W#2), the second sample is a piece of bulk W with fuzz-like nanostructures were produced on it using a pure 37 keV He beam and a fluence of 1x10^{24} 1/m^2 in the GLADIS facility [20] (T#3), and the third sample a milled graphite with a 20 nm W coating (M#2). The position of samples on the AUG divertor manipulator arm together with the strike point are shown in Figure 1c.

In the case of the ^{15}N experiment, the main focus was on deposition of nitrogen, thus the surfaces needed to be fully covered with W. In contrast, in the He experiment, more emphasis was put on erosion characteristics of W, and this required that the coatings should not be too thick. Those lead to difference in sample composition from both experiments. The summarised composition of all the exposed samples and the properties of the AUG discharges are presented in Table 1.

For microbeam measurements we used the 2 MV tandem accelerator at Jožef Stefan Institute [9] coupled with a microbeam line, located at 10° from the exit port of the accelerator. The accelerator and the beam line are coupled with a high brightness multicusp ion source for producing a high brightness proton ion beam [10], which can be focused to dimensions down to 0.5x0.5 μm^2 at the energy of 3 MeV in a high current mode [11]. Light Z elements (Z<9) are generally detected by nuclear reaction analysis (NRA). To quantify the amount of D the D(^{3}He,p)α nuclear reaction was used [12,13]. We focused a 3.3 MeV ^{3}He ion beam down to 10x10 μm^2 in a high current mode of 300 pA. For NRA measurements of ^{11}B and ^{15}N, which were quantified by the nuclear reactions ^{11}B(p,α)^{8}Be [14,15] and ^{15}N(p,α)^{12}C [16], we used a focused proton beam at energies of 2.6 MeV and 1 MeV respectively. Both beams were focused down to 1.5x1.5 μm^2 in the high current mode. The dimensions of the ion beam are optimized with a knife edge method on a copper grid, using induced K_α X-ray emission and HP-Ge X-ray detector.

For the quantification of the measurement data of ^{11}B and ^{15}N, we used the cross sections available for these two nuclear reactions and compared the simulated signals to the experimental ones obtained from the calibrated boron and nitrogen standards. For B, an amorphous boron hydride (a-B:H, with B amount of 3x10^{18} B/cm^2 and H amount of 8x10^{17} H/cm^2) was used as standard while for the ^{15}N standard, a sample with 3x10^{16} at/cm^2 of ^{15}N implanted into W was used.

The end station is equipped with a 5-axes manipulator and a microscope with a camera for sample positioning in the focal plane of the ion beam. In front of the end station a triplet of quadrupole magnetic lenses is used for focusing the ion beam and deflection coils for rastering the beam on the sample. With existing hardware, we are able to scan the beam across an area of 2200x2200 μm^2 and

produce elemental maps with a resolution of 256x256 pixels. For dose normalization we use a beam chopper combined with an RBS detector [17]. A high-purity germanium X-ray detector is positioned at 135° with respect to the beam direction. It is used to reveal the concentrations and distribution of various metallic impurities on the samples by particle induced X-ray emission (PIXE) measurements. The detector is optimized for the detection of X-rays in the region from 3 to 54 keV. To study the possible layered structure of the analyzed samples, an RBS detector with a 300 μm thick depletion layer is positioned at 135° with respect to the beam direction, covering a solid angle of 5.6 msr. It is equipped with a 0.8 μm thick Al foil serving as a light block filter. For spectroscopy of the fast protons emitted from the nuclear reactions a NRA detector is positioned at 135° with respect to the primary beam direction. The NRA detector has a 1000 μm thick depletion layer with an active area of 300 mm^2. At the mounted position the detector covers a solid angle of 0.14 sr. The detector is shielded by a thin Al foil which serves as visible light block. For the detection of fast protons emitted in the D(^{3}He,p)^{4}He reaction we used 6 μm of Al foil and 125 μm thick kapton foil while for the B and N reactions we used only 3 μm thick Al foil. This combination of foils also produces enough energy loss for the fast protons, to be completely stopped in the depleted layer of the NRA detector and is thick enough to stop the backscattered ions (protons or ^{3}He) from the primary beam. The acquisition system is designed in a way that each detector event in the set of detectors is recorded and saved in a list mode together with the information on the beam position. More details on the experimental set up are given in Ref. [4].

The microbeam analysis on samples from ^{15}N experiment consisted of 3 rectangular measurement spots across the poloidal direction at equidistant steps of 14.75 mm; along this line the changes in the plasma conditions during the exposure in AUG were the largest. The scanned areas are shown in Figure 1b for one of the samples from the ^{15}N experiment. The samples from the He experiment were only analysed with a 2.6 MeV proton beam, as the main focus was the analysis of B as impurity by the ^{11}B(p,α)^{8}Be reaction. The scanned areas in the case of M#2 and T#3 samples are shown in Figure 1d. To obtain the poloidal elemental profiles the measured 2D maps were projected along the line of interest. The obtained NRA and RBS spectra were analysed with the SIMNRA [18] program to calculate the concentrations of different elements. PIXE spectra were analysed using the GeoPIXE software [19] and errors of the obtained concentrations are estimated to be below 15%, which manly originate from inaccuracy of the fitting and finite precision of the ion current measurements.

3. Results

In the section 3.1 we are going to present and discussed results obtained from the ^{15}N experiment and in section 3.2 results from the He experiment.

3.1 Results from ^{15}N experiment

Two examples, of a detailed 2D deuterium distribution maps from the samples M2 and P2 are shown in Figures 2a and 2b, respectively. In order to decrease statistical scattering in the D map, the bunches of image pixels were merged, resulting in the statistical error to be reduced below 10%. The lateral

distribution of D along the poloidal axis for all analysed AUG samples from the ^{15}N experiment is shown in Figure 2c. The D amount is on average 80-90x10^{15} D/cm^2 for milled graphite (M) samples, 30-40x10^{15} D/cm^2 for polished (P) graphite samples and 10-15x10^{15} D/cm^2 for W bulk sample. There is a clear trend of D retention to increase with increasing surface roughness. We also observed a small dependence of D retention on the analysing position, obtaining the largest retention on both sides (below and above) near the strike point, the location of highest impinging ion and impurity flux.

Detailed 2D distribution maps for ^{15}N are shown on Figures 3a and 3b, also for M2 and P2 samples. The distribution of the ^{15}N along the poloidal axis for all analysed samples is shown in Figure 3c. The average ^{15}N amounts are 5-13x10^{15} N/cm^2 as shown on Figure 3 and are comparable to those obtained in Ref. [6]. As observed for the deuterium retention also the largest ^{15}N content is obtained for the milled graphite sample. On bulk W samples the impurity retention is the lowest being 3-7x10^{15} N/cm^2. The 2D distribution maps for D and ^{15}N show no direct correlation of the hot spots on a micrometre level. Due to the low counting statistics for boron we could not reproduce the 2D distribution maps, therefore we show only the lateral distribution of B for the analysed samples in Figure 4. The B amount is between 20x10^{15} B/cm^2 and 30x10^{15} B/cm^2 for the three types of samples.

The profiles of the retained D and ^{15}N, on milled and polished samples, show similar profiles in poloidal direction with peak values occurring above the strike point. Both profiles differ in regions away from the strike point in the scrape-off layer. The D profile show first slight decrease and then increase even further off from the strike point. In contrast, ^{15}N is distributed homogenously in this regions. The same behaviour for ^{15}N deposition is observed for the bulk W sample while now D is distributed much more homogenously than on the different graphite samples. In general we observe a slight increase of D and ^{15}N in the regions further from the strike point, while ^{11}B is decreased in the same regions. The ^{11}B distribution can be explained by B originating from the residual B inventories inside the vessel while D and N were directly injected during the discharges. The variations of ^{15}N and ^{11}B along the poloidal direction agree with the measurement obtained with the broad beam measurements [6]. We observed some W surface scratches in poloidal direction, probably due to arc traces on the surface which cannot be correlated with impurity distributions. Other heavy impurities were measured by the PIXE technique and found to be homogenously distributed over the polished and unpolished graphite samples yielding around 2x10^{15} Ca/cm^2 of Ca, 1x10^{15} Ti/cm^2 of Ti, 1x10^{15} Cr/cm^2 of Cr and 8x10^{15} Fe/cm^2 of Fe . In bulk W samples we detected only around 1x10^{15} Fe/cm^{2}of Fe while Ca, Ti and Cr were below the detection limit.

3.2 Results for He experiment

Analysed samples from the He experiment show inhomogeneous distribution of W with micro-scale roughness which is most pronounced on W coated sample (M#2) and on pre-damaged sample (T#3) where the fuzz-like structure is visible on Figure 5a) and b). The structures on the M#2 sample originate from sample preparation, as discussed in Kelemen et al. [4]. The surface features on the T#3 sample are produced by exposure in GLADIS. On Figure 5 we show SEM images for the two samples and PIXE elemental maps of W, which correlate well with each other. On the layered sample (M#2)

we observe a similar surface structure of W, having a shape of snake skin as reported in [4], which shows no correlation to the impurity deposition profiles on micrometre scale.

In Figures 6a and 6b detailed 2D distribution maps of ^{11}B are shown for M#2 and T#3 samples, respectively. The lateral distributions of B for all three samples at different analysing position along the poloidal axis are shown in Figure 6c, and show some increase of retained ^{11}B above strike point. The retention of ^{11}B is the strongest in the pre-damaged sample (T#3) ranging between 2000-3500 x10^{15} B/cm^2, while the B amount on W deposited on graphite (M#2) and bulk W (W2) is 450-600 x10^{15} B/cm^2 and around 100 x10^{15} B/cm^2 respectively, as shown in Figure 6. The ^{11}B amounts on the samples from the He experiment are substantially higher than in the case of the ^{15}N experiment. The reason for this difference lies in the time sequence the way experiments were carried out. The He experiment was carried out shortly (days) after the boronization of the AUG. The He experiment was carried out shortly (days) after the boronization of the AUG vessel where on the other hand the ^{15}N experiment was performed long after the boronization. One more reason for the increased B amount in the He experiment could be due to the He plasma discharge being more efficient in removing deposits from the main chamber and depositing them in the divertor region. For pre-damaged W sample we observe also large increase of heavy impurities like Ti, Cr and Fe yielding concentrations of 470 x10^{15} Ti/cm^2, 32 x10^{15} Cr/cm^2, 97 x10^{15} Fe/cm^2, respectively, as compared to bulk W sample where Ti, Cr and Fe are almost on the detection limit (21 x10^{15} Ti/cm^2, 9 x10^{15} Cr/cm^2, 29 x10^{15} Fe/cm^2). Also higher amounts of impurities were observed in M#2 sample, 27 x10^{15} Ti/ cm^2, 4 x10^{15} Cr/cm^2 and 27x10^{15} Fe/g . All the surface features (seen in the W PIXE maps) and scratches on samples cannot be correlated to the ^{11}B distribution.

3.3 Comparing the ^{15}N and He experiments Comparing the B distribution on rougher samples from ^{15}N and He experiments(M2, P2, M#2 and T#3), we observe difference in their characteristics. On samples from ^{15}N experiment we observe increase of ^{11}B deposition to increase below strike point and reach minimum above it. On the other hand in the He experiment ^{11}B is distributed homogeneously (on micrometre level), while on larger scale we observe increase above the strike point. For bulk W samples from both experiments we do not see any large variation in B profiles.

In both experiments we did not observe great topological effects on impurity retention on micrometre scale only an small variation of retained impurities.

Summary

We have analysed W and W deposited on graphite samples exposed in the ASDEX Upgrade tokamak, during experiments where ^{15}Nwas injected into L-mode discharges in D and during non-seeded H-mode discharges in He. Focused MeV ion beams with micro-meter lateral resolution were applied in these analyses. The main focus was on the use of nuclear reaction analysis for the detection of D, ^{11}B and ^{15}N.

For the samples exposed in the ^{15}Nseeded plasma we observe a slight increase of retained D and ^{15}N in the regions further from strike point and decrease of ^{11}B in the same regions. This behaviour is

attributed to the fact that the ^{11}B is a residual impurity, being retained in the private flux region from the boronization, while D and ^{15}N were actively introduced and migrated also around the strike point. On the micro-scale we observe a small variation in impurity distribution inside of the scanned areas. We observed some difference of the retained impurities between different types of samples. We found an increased retention on samples with W deposited on graphite base as compared to bulk W samples. Most of the differences in the impurity deposition densities are associated with the sample roughness: bulk W being very smooth, followed by sample with the polished graphite substrate, and finally sample with deposited W on unpolished graphite with highest roughness, featuring the highest impurity deposition and highest fuel retention.

On pre-damaged W bulk sample from the He experiment we observed some W fuzz-like structures on the sample surface which cannot be correlated with the distribution of other impurities. On the sample with W coated on graphite we observe some W hot spots on the surface. In addition, bulk W samples show nonhomogeneous distribution of impurities on the surface.

From our result we can make a general conclusion that rougher surfaces are more susceptible for retention of fusion fuel and other impurities.

Acknowledgments

This work has been carried out within the framework of the EUROfusion Consortium and has received funding from the Euratom research and training programme 2014-2018 under grant agreement No 633053. Work was performed under EUROfusion WP PFC and exposure experiments carried out under WP MST1 . The views and opinions expressed herein do not necessarily reflect those of the European Commission.

References

[1] M. Mayer et al., J. Nucl. Mater. 363-365 (2007) 101-106
[2] H. Khodja et al., Nucl. Instr. Meth. B 266 (2008) 1425
[3] P. Petersson et al., Nucl. Instr. Meth. B 268 (2010) 1833
[4] M. Kelemen et al., Nucl. Instr. Meth. B 2017 in press, https://doi.org/10.1016/j.nimb.2017.01.072
[5] A. Herrmann et al., Fusion Eng. Des. 98-99 (2015) 1496
[6] G. Meisl et al., Nucl. Mater. Energ. 2016 in press, https://doi.org/10.1016/j.nme.2016.10.023
[7] S. Brezinsek et al., Nucl. Mater. Energ. 2016 in press, https://doi.org/10.1016/j.nme.2016.11.002
[8] A. Hakola et al., Nucl. Fusion 57 (2017) 066015
[9] P. Pelicon et al., Nucl. Instr. Meth. B 269 (2011) 2317
[10] P. Pelicon et al., Nucl. Instr. Meth. B 332 (2014) 229
[11] P. Vavpetič et al., Nucl. Instr. Meth. B 2017 in press, https://doi.org/10.1016/j.nimb.2017.01.023
[12] M. Mayer et al., Nucl. Instr. Meth. B 267 (2009) 506
[13] S. Markelj et al., J. Nucl. Mater. 469 (2016) 133
[14] M. Mayer et al., Nucl. Instr. Meth. B 143 (1998) 244-252
[15] M. Kokkoris et al., Nucl. Instr. Meth. B 268 (2010) 3539-3545

[16] F. B. Hagedorn et al., Phys. Rev. 108, 4 (1957) 1015
[17] K. Vogel-Mikus et al., Nucl. Instr. Meth. B 267 (2009) 2884
[18] M. Mayer, SIMNRA User's Guide: Report IPP 9/113, Max-Planck-Instutut für Plasmaphysik Garching, 1997.
[19] C. G. Ryan et al., Nucl. Instr. Meth. B 363 (2015) 42
[20] H. Greuner et al., Fusion Eng. Des. 75-79 (2005) 345-350

List of figure captions

Fig.1: a) A photo of the samples mounted on the divertor manipulator arm in the ^{15}N experiment in AUG.
b) A photo of one of the exposed samples with marked regions (white rectangles) of the performed analysis using ion beam techniques by microbeam.
c) A photo of the samples mounted on the divertor manipulator arm in the He experiment in AUG.
d) A photo of two of the exposed samples where the regions of analysis using microbeam techniques are marked by white rectangles.

Fig.2: The D amounts for two samples exposed in AUG tokamak in ^{15}Nseeding campaign: a) and b) 2D maps of D distribution with 366 μm resolution on M2 and P2 samples, respectively; c) The amounts of D plotted in the poloidal direction for all analysed samples.

Fig.3: The N amounts for two samples exposed in AUG tokamak in ^{15}N seeding campaign: a) and b) 2D maps of N distribution with 157 μm resolution on M2 and P2 samples, respectively; c) The N amounts plotted in the poloidal direction for all analysed samples.

Fig.4: The B amounts for the samples exposed in AUG tokamak in ^{15}N seeding campaign plotted in poloidal direction for all analysed samples.

Fig.5: Maps of W X-ray yield obtained by PIXE with 2.6 MeV protons a) sample of 20 nm of W deposited on graphite (M#2) and b) pre-damaged bulk W samples (T#3) both from AUG He experiment.
The secondary electron SEM image of c) sample of 20 nm of W deposited on graphite (M#2) and d) pre-damaged bulk W samples (T#3). The SEM images were done at Center electron microscopy and microanalysis (CEMM) of Jožef Stefan Institute.

Fig.6: The^{11}B amounts for the samples exposed in AUG tokamak in the He experiment: a) and b) show 2D maps of ^{11}B distribution with 157 μm or 75 μm (finer maps) resolution on M2 and T3 samples, respectively c) the amount of ^{11}B plotted in the poloidal direction for all analysed samples is shown.

List of table captions

Table 1: Summary of sample types and exposures in AUG. The number of the sample name corresponds to the location on the AUG manipulator arm during the exposure.

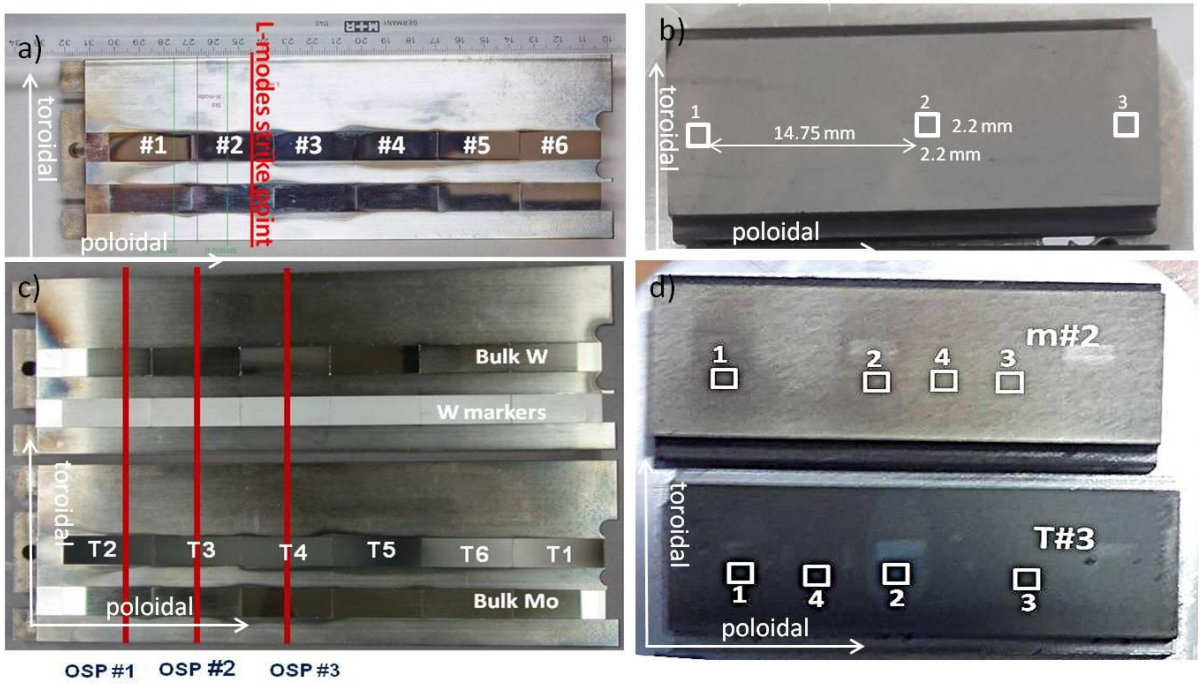
a)
toroidal
poloidal
L-modes strike point
#1
#2
#3
#4
#5
#6
b)
toroidal
poloidal
1
2
3
14.75 mm
2.2 mm
2.2 mm
c)
Bulk W
W markers
toroidal
poloidal
T2
T3
T4
T5
T6
T1
Bulk Mo
OSP #1
OSP #2
OSP #3
d)
m#2
1
2
4
3
toroidal
poloidal
T#3
1
4
2
3

Figure 1

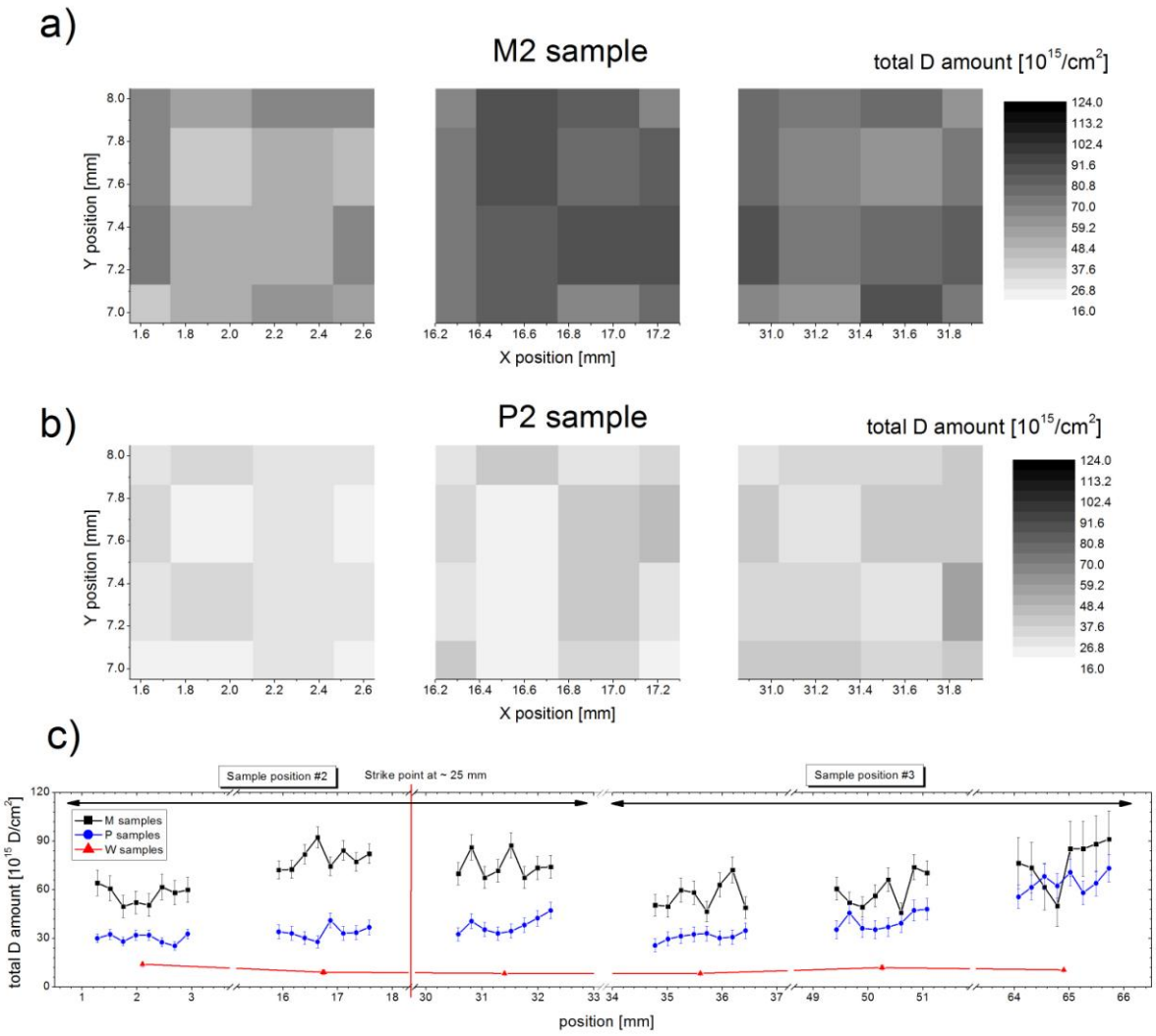
a)
M2 sample
total D amount [10^15/cm^2]
Y position [mm]
X position [mm]
b)
P2 sample
total D amount [10^15/cm^2]
Y position [mm]
X position [mm]
c)
Sample position #2
Strike point at ~ 25 mm
Sample position #3
M samples
P samples
W samples
total D amount [10^15 D/cm^2]
position [mm]

Figure 2

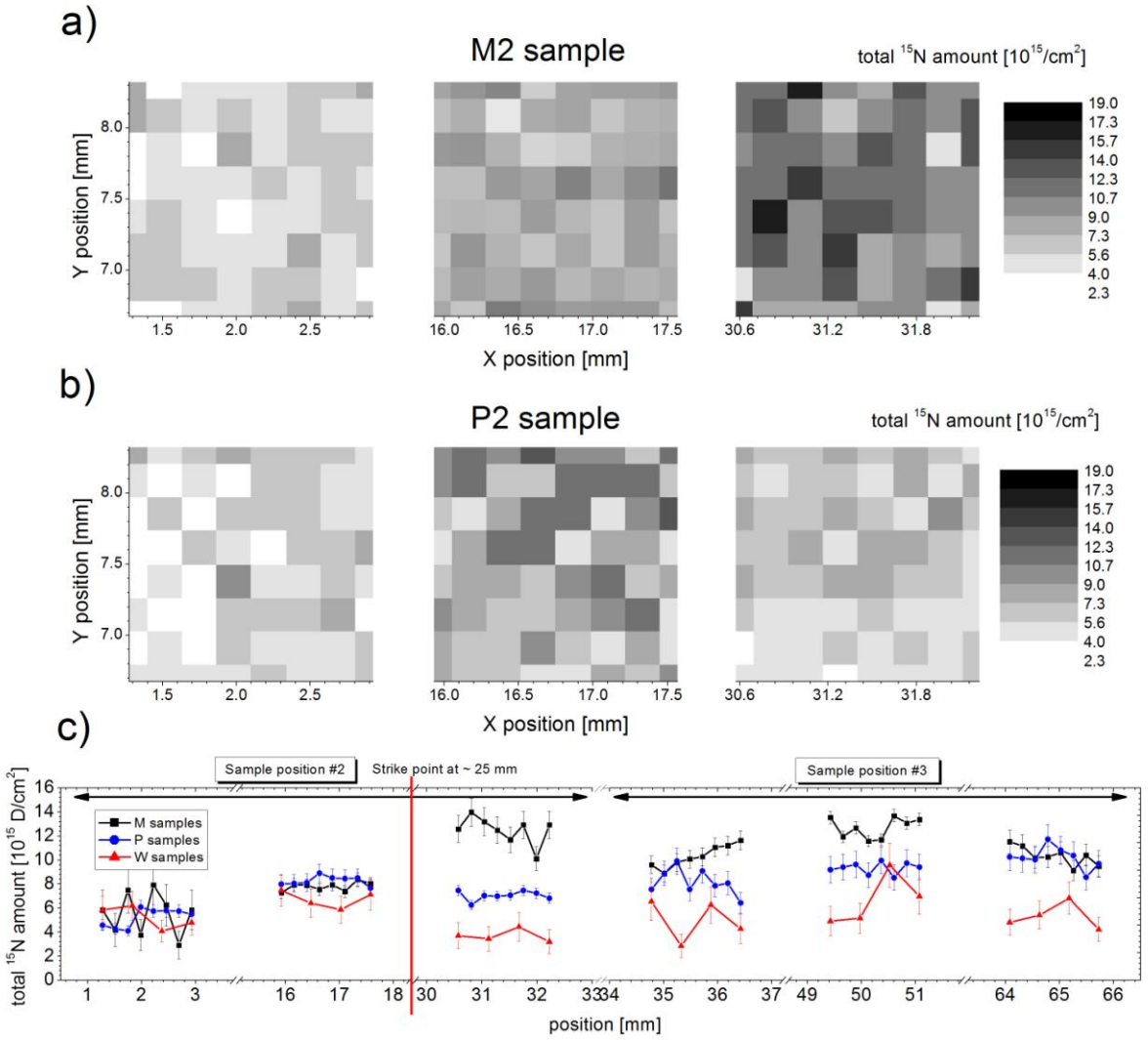
a)
M2 sample
total ^{15}N amount [10^{15}/cm^2]
Y position [mm]
X position [mm]
b)
P2 sample
c)
Sample position #2
Strike point at ~ 25 mm
Sample position #3
M samples
P samples
W samples
total ^{15}N amount [10^{15} D/cm^2]
position [mm]

Figure 3

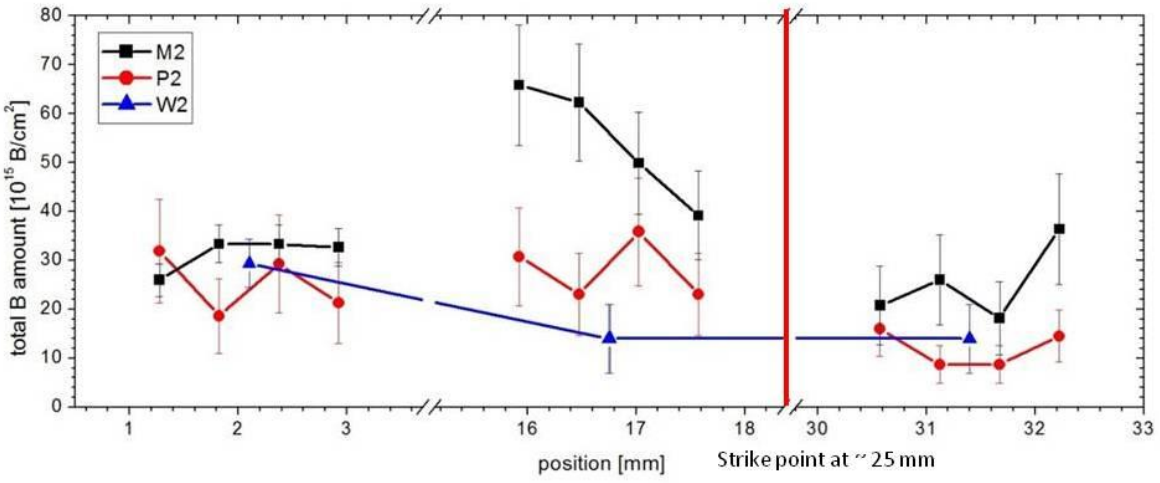
M2
P2
W2
total B amount [10^15 B/cm^2]
position [mm]
Strike point at ~ 25 mm

Figure 4

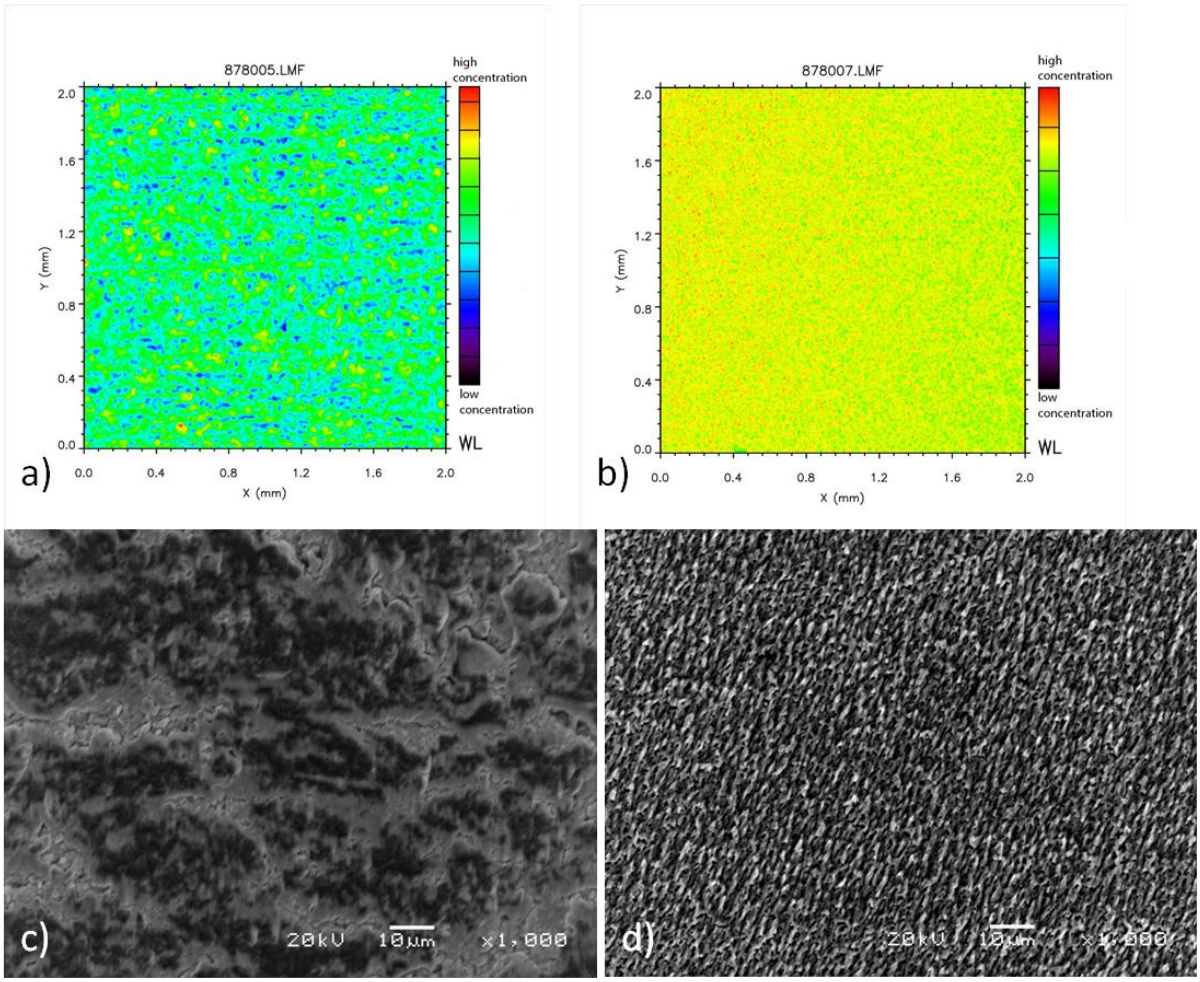
878005.LMF
high concentration
low concentration
WL
Y (mm)
X (mm)
a)
878007.LMF
high concentration
low concentration
WL
Y (mm)
X (mm)
b)
c)
20kV 10µm ×1,000
d)
20kV 10µm ×1,000

Figure 5

326

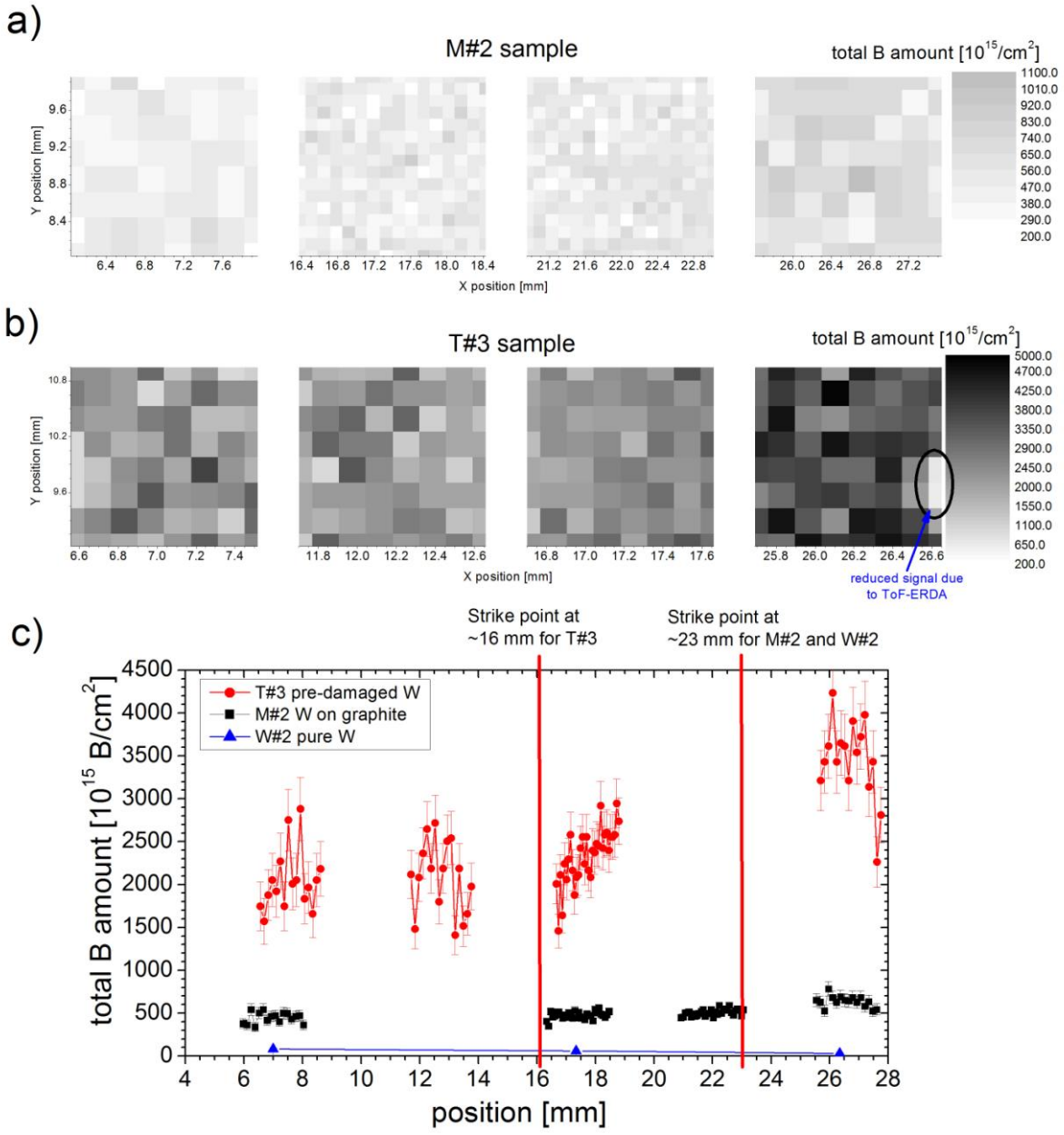
a)
M#2 sample
total B amount [10^15/cm^2]
Y position [mm]
X position [mm]
b)
T#3 sample
total B amount [10^15/cm^2]
Y position [mm]
X position [mm]
reduced signal due to ToF-ERDA
c)
Strike point at ~16 mm for T#3
Strike point at ~23 mm for M#2 and W#2
T#3 pre-damaged W
M#2 W on graphite
W#2 pure W
total B amount [10^15 B/cm^2]
position [mm]

Figure 6

327

Sample	Composition	Surface roughness	Exposure in AUG	Seeding
M 2/3	Milled graphite with 100 nm of W coating	~1 μm	5 L-mode discharges in D	$5.3x10^{21}$ ^{15}N atoms
P 2/3	Polished graphite with 100 nm of W coating	~0.3 μm	5 L-mode discharges in D	$5.3x10^{21}$ ^{15}N atoms
W 2/3	Bulk polished W	<0.1 μm	5 L-mode discharges in D	$5.3x10^{21}$ ^{15}N atoms
T#3	Bulk W, exposed to $1x10^{24}$ m^{-2} of 37 keV He atoms in GLADIS	>1 μm	9 H-mode discharges in He and H	Non seeded
M#2	Milled graphite with 20 nm of W coating	~1 μm	9 H-mode discharges in He and H	Non seeded
W#2	Bulk polished W	~<0.1 μm	9 H-mode discharges in He and H	Non seeded

Table 1